

Design of a 3D-printed hand prosthesis featuring articulated bio-inspired fingers

Cuellar Lopez, J.S.; Plettenburg, Dick; Zadpoor, Amir A.; Breedveld, Paul; Smit, Gerwin

DOI

[10.1177/0954411920980889](https://doi.org/10.1177/0954411920980889)

Publication date

2021

Document Version

Final published version

Published in

Proceedings of the Institution of Mechanical Engineers, Part H: Journal of Engineering in Medicine

Citation (APA)

Cuellar Lopez, J. S., Plettenburg, D., Zadpoor, A. A., Breedveld, P., & Smit, G. (2021). Design of a 3D-printed hand prosthesis featuring articulated bio-inspired fingers. *Proceedings of the Institution of Mechanical Engineers, Part H: Journal of Engineering in Medicine*, 235 (3), 336-345.
<https://doi.org/10.1177/0954411920980889>

Important note

To cite this publication, please use the final published version (if applicable).
Please check the document version above.

Copyright

Other than for strictly personal use, it is not permitted to download, forward or distribute the text or part of it, without the consent of the author(s) and/or copyright holder(s), unless the work is under an open content license such as Creative Commons.

Takedown policy

Please contact us and provide details if you believe this document breaches copyrights.
We will remove access to the work immediately and investigate your claim.

Green Open Access added to TU Delft Institutional Repository


'You share, we take care!' - Taverne project

<https://www.openaccess.nl/en/you-share-we-take-care>

Otherwise as indicated in the copyright section: the publisher is the copyright holder of this work and the author uses the Dutch legislation to make this work public.

Design of a 3D-printed hand prosthesis featuring articulated bio-inspired fingers

Juan Sebastian Cuellar¹, Dick Plettenburg, Amir A Zadpoor, Paul Breedveld and Gerwin Smit¹

Proc IMechE Part H:
J Engineering in Medicine
2021, Vol. 235(3) 336–345
© IMechE 2020
Article reuse guidelines:
sagepub.com/journals-permissions
DOI: 10.1177/0954411920980889
journals.sagepub.com/home/pih


Abstract

Various upper-limb prostheses have been designed for 3D printing but only a few of them are based on bio-inspired design principles and many anatomical details are not typically incorporated even though 3D printing offers advantages that facilitate the application of such design principles. We therefore aimed to apply a bio-inspired approach to the design and fabrication of articulated fingers for a new type of 3D printed hand prosthesis that is body-powered and complies with basic user requirements. We first studied the biological structure of human fingers and their movement control mechanisms in order to devise the transmission and actuation system. A number of working principles were established and various simplifications were made to fabricate the hand prosthesis using a fused deposition modelling (FDM) 3D printer with dual material extrusion. We then evaluated the mechanical performance of the prosthetic device by measuring its ability to exert pinch forces and the energy dissipated during each operational cycle. We fabricated our prototypes using three polymeric materials including PLA, TPU, and Nylon. The total weight of the prosthesis was 92 g with a total material cost of 12 US dollars. The energy dissipated during each cycle was 0.380 Nm with a pinch force of ≈ 16 N corresponding to an input force of 100 N. The hand is actuated by a conventional pulling cable used in BP prostheses. It is connected to a shoulder strap at one end and to the coupling of the whiffle tree mechanism at the other end. The whiffle tree mechanism distributes the force to the four tendons, which bend all fingers simultaneously when pulled. The design described in this manuscript demonstrates several bio-inspired design features and is capable of performing different grasping patterns due to the adaptive grasping provided by the articulated fingers. The pinch force obtained is superior to other fully 3D printed body-powered hand prostheses, but still below that of conventional body powered hand prostheses. We present a 3D printed bio-inspired prosthetic hand that is body-powered and includes all of the following characteristics: adaptive grasping, articulated fingers, and minimized post-printing assembly. Additionally, the low cost and low weight make this prosthetic hand a worthy option mainly in locations where state-of-the-art prosthetic workshops are absent.

Keywords

3D printing, hand prostheses, bio-inspired design, mechanical design, biomedical devices

Date received: 28 April 2020; accepted: 17 November 2020

Introduction

The demand for prosthetic limbs is rising as the number of amputations is increasing worldwide. In the United States alone, it is estimated that 185,000 amputations are performed every year.¹ The demand for upper limb prostheses is important since a relevant percentage of all limb loss cases are related to the upper limb(s). In the United States a total of 41,000 cases of trans-radial and trans-humeral amputations were estimated in 2005.² The after-effects of an upper limb loss can be devastating both for the mental and physical

well-being of the amputee. Designing and fabricating an upper limb prosthesis is therefore essential in order

Department of Biomechanical Engineering, Faculty of Mechanical, Maritime and Materials Engineering, Delft University of Technology, Delft, The Netherlands

Corresponding author:

Juan Sebastian Cuellar, Department of Biomechanical Engineering, Faculty of Mechanical, Maritime and Materials Engineering, Delft University of Technology, Mekelweg 2, Delft, 2600 AA, The Netherlands.
Email: J.S.CuellarLopez@tudelft.nl

to help amputees to recover functionality and increase their quality of life.³

The ultimate goal of prosthetic devices is to mimic the functionality of a missing body part. Unfortunately, the complexity of anatomic structures in a real hand is such that prosthetic designs have to be simplified to facilitate fabrication with current technologies. In this context, designers tend to disregard biological principles, instead opting for existing conventional design methods that they are confident would work and provide partial functionality of the missing body part. These conventional approaches guide the design process of most of the prosthetic hands found in the literature. The designers will, in most cases, use standard parts and mechanisms such as helical springs, screws, cables, etc. Examples of such designs are reviewed in the work of Belter et al.⁴ including descriptions of a number of mechanical specifications. Many working principles of a number of anatomical structures, like finger pads, ligaments, tendons or skin that could improve the performance of current hand prostheses, are usually not present in their designs.^{4,5} One simple example is to include sliding joints similar to the ones found in the human finger instead of conventional hinged joints.

3D printing is a relatively new, rising technology that facilitates the manufacturing of parts with irregular and uncommon geometric shapes.⁶ The form-freedom offered by 3D printing techniques has paved the way for the application of new design approaches; for example the non-assembly design approach.^{7,8} Current 3D-printed hands are based on a mechanical inspired design, rather than a biological inspired design. Previous hand prostheses produced by 3D printing are typically articulated by hinged joints, are assembled with screws and driven and stabilized by cables or mechanical linkages.^{9–14} Others have rather opted for 3D printed compliant mechanisms such as joints and/or extensors of the fingers,^{8,15–17} but still using conventional driving mechanisms. Bio inspiration then serves as design alternative founded on the idea that biological designs are different, and that in this difference new and smart solutions can be found that we do not find in conventional technical approaches. By studying something that is entirely different, gateways to other worlds of solutions can be opened expanding creativity. Bio-inspiration is not about simply copying these other worlds, but about using this knowledge to find new combinations of solutions that could be better as compared to solutions just drawn from pure technical backgrounds. A few examples originating from this include biarticular actuators by Sharbafi et al.,¹⁸ a rolling robot by Lin et al.,¹⁹ a micro air vehicle by Nguyen and Chan²⁰ and a surgical steerable needle by Scali et al.²¹ In the same way, following a design approach inspired by human anatomy could improve the performance of prosthetic hands.

The advantages of 3D printing could be used to fabricate advanced, yet simple to print, prosthetic hands

based on the biological design principles in human hands. A bio-inspired design approach could be a more practical way of incorporating new beneficial features into a prosthetic hand instead of mimicking the biological structures with synthetic materials. In this study, we therefore aimed to identify working principles in the human hand that can be included in a new prosthetic hand using 3D printing technology. We then applied a bio-inspired approach to the design and fabrication of articulated fingers that allows for the execution of multiple grasping patterns.

The human finger

Our bio-inspired design approach started with the study of the biological assembly of the human finger: the bones (links) and the structures that connect them (joints). We then continued with an analysis of the anatomic elements for force and motion control in order to devise the transmission and actuation system (i.e., muscles, tendons, anatomical pulleys, and tendon sheaths). Structures such as the nerves and veins are out of the scope of this study, because their function is not directly related to the mechanical performance of the finger. A human finger consists of four rigid bones, starting from proximal to distal, the metacarpal (MC), proximal phalanx (PP), middle phalanx (MP), and distal phalanx (DP). The interconnecting joints are the metacarpophalangeal (MCP) joint, the proximal interphalangeal (PIP) joint, and the distal interphalangeal (DIP) joint. Two different forms of joints can be distinguished in this regard: hinged joints that permit flexion/extension and ellipsoid joints that also allow for adduction/abduction (rotation around the dorsal-palmar direction). This corresponds to 1 degree of freedom (DoF) at the PIP and DIP joints (hinged) and 2 DoF at the MCP joint (ellipsoid), respectively. More distinctively, in the hinged joints, there is a tongue along the convex surface and a groove along the concave surface of the joint, this helps to prevent lateral translation (Ulnar-Radial directions, see Figure 1).²²

Ligaments connect the bones of the hand to one another. Their main role is to stabilize the joints and constrain the range of motion of the bones. The *collateral ligaments* are found on the lateral sides of the joints, see Figure 1; the proper ligament is attached eccentrically with the shape of a cord and the accessory ligament initiates from the center of rotation of the proximal side of the joint and is fixed to the palmar plate in a fan shape. These two ligaments restrict translation of the bones to the distal direction of the finger and also movement to the Ulnar-Radial direction,²² see Figure 1.

The muscles can be considered to be the actuators of the finger, while the tendons are the structures that transmit the force of the muscles to the bones. Two groups of muscles and tendons are primarily used for the flexion of the fingers, namely the flexor digitorum profundus (FDP) and the flexor digitorum superficialis

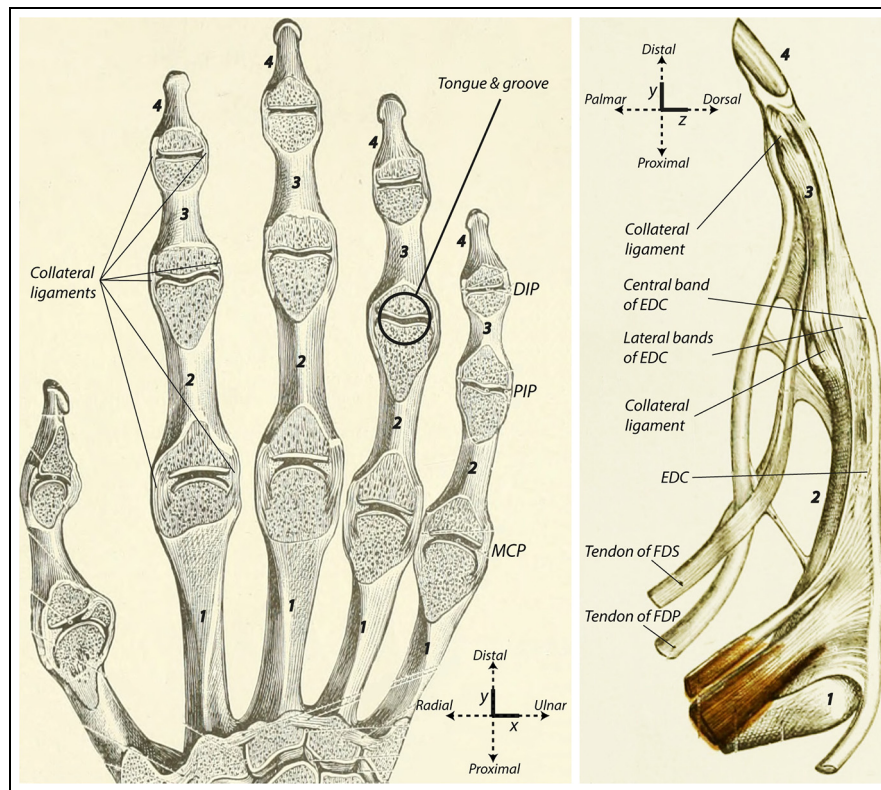


Figure 1. Anatomy of the finger. (Left) Dorsal aspect of the bones of the human hand. The metacarpophalangeal (MCP) joint, the proximal inter-phalangeal (PIP) joint, the distal inter-phalangeal (DIP) joint, the tongue and groove configuration inside the joints and collateral ligaments are shown. (Right) Ulnar aspect of the middle finger of the human hand. Also shown: The tendons of the flexor digitorum profundus (FDP) and the flexor digitorum superficialis (FDS), the central and lateral bands of the extensor digitorum communis (EDC) and collateral ligaments. For both images: (1) metacarpal bone (MC), (2) proximal phalanx (PP), (3) middle phalanx (MP), and (4) distal phalanx (DP) are identified; anatomical directions can be seen at the bottom right corner (left) and upper left corner (right). Modified and reprinted from Toldt et al.²³ under a CC BY license.

(FDS), see Figure 1. The FDP is the main flexor. The FDS contributes to exert larger forces when the FDP is not providing sufficient force. The mechanical configuration of the finger is therefore underactuated (more DoF than actuators) during the flexion of the human finger (3 DoF, 2 actuators). The central band of the extensor digitorum communis (EDC) has the principal role of extending the MCP joint. The lateral bands of the EDC have two functions depending on the position of the bands with respect to the center of rotation of the joint: they can either aid to extend or flex the PIP and DIP joint. As the phalanges move, the bands of the EDC move to the other side of the center of rotation providing a moment to the opposite direction and favoring the flexion of the joints.²² Interestingly, the flexor and extensor tendons inside the hand have different cross-sectional area shapes depending on the function and location. For example, the tendons of the FDS have an oval shape over the region of the MCP joint, they flatten close to the middle of the PP and then it splits into halves.²⁴

The sheaths and pulleys form a kind of ‘tunnel’ that keeps the tendons in place and constrains their excursion. They fulfil the role of keeping the force delivered by the flexor muscles perpendicular to the center of

rotation of the joint.²⁵ Sheaths are located over the anterior side of the finger and prevent the dislocation of the extensor tendon. On the palmar side, fibrous sheaths enclose the finger along its full length. A sequence of flexible bands strengthens the fibrous sheaths at intervals forming the pulleys.²⁶

Design of the prosthetic hand

Simplifications for applications in body powered (BP) hand prostheses

We continued our design by establishing a number of basic (*i.e.*, functional) requirements for the hand prosthesis based on the work by Plettenburg²⁷: body-powered (BP) control, cosmetic appearance, light weight, and water/dirt resistance (materials resisting any contact with water and dirt). A number of simplifications as compared to the human hand are therefore considered in order to fulfil these criteria.

BP hand prostheses use a single driving input to activate the grasper. Individual finger control or multi-degree of freedom thumb control are thus not feasible; to comply with this requirement we decided for a static thumb and four active fingers for the grasping action.

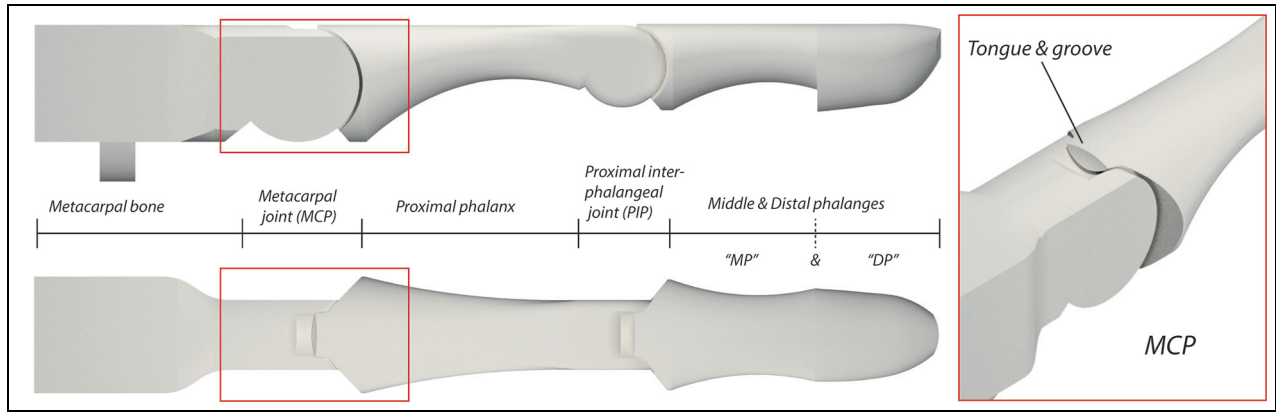


Figure 2. The design of the links of the prosthetic finger.

The movement of the active fingers can then be controlled by a single driving link. This means that there is one movement available, which is the simultaneous closing of the four fingers. Furthermore, natural under-actuation during the flexion of the human finger (3 DoF, 2 actuators) must be simplified to a single actuator as well. Moreover, the number of DoF per finger in the human hand is problematic from a mechanical design standpoint, as every joint adds a force loss associated with friction. We therefore decided to reduce the number of DoF per finger from three to two by combining the distal and medial phalanges into a single link. As a result, each finger can be driven by a single tendon-based transmission system guided by two rigid pulleys connected at the end of each joint. In this way, the FDP and FDS are merged into a single muscle-tendon system. At the same time, force can be distributed to all fingers using a whiffle tree configuration similar to our previous design.⁸ The pulley system is simplified to only three annular pulleys per finger (one per joint and one over the MC bone), since extra guiding elements would increase the contact points of the driving tendon and thus the friction associated with its activation. In contrast with the biological counterpart, lubricant fluids are not considered. The complex structure of tissues that holds the joints in position is also reduced to spring-like elements that constrain the motion to only one rotational DoF, that is flexion/extension.

Working principles

The shape of the links and joints is based on the shape of the human bone phalanges. The joints are designed as circular hinged joints including a tongue and groove contact at the centre of the lateral plane along the radial line of the joint (Figure 2), thereby restricting the lateral motion. The MCP joint is larger compared to the PIP joint. The moment arm that can be exerted with the driving cable is therefore larger at the MCP joint. A reduction of the cross-sectional area of the phalanges can be seen towards the centre, allowing for additional

space where parts of the driving mechanism can be placed. The nominal size of the links is set to the average size of human bones of a sample of 253 males in the USA, as described in the work of Vicinus.²⁸ The size of the palm and thumb are also based on this work. The total weight of the prostheses must be below 400 g, which is below the average weight of a human hand.²⁹

The parts that return the phalanges to a straight position are flexible strips that provide a spring-like behavior. These elements can be easily bent and stretched within the elastic region of the material and are designed similar to the biological configuration of the EDC tendons over the PIP joint, one central strip running above the dorsal side of the bones and two lateral strips, one along the ulnar direction and the other along the radial direction of the bones (Figure 3, *top*). As the phalanges bend, the lateral flexible strips stretch, following a trajectory that reduces the moment arm to the centre of rotation (Figure 3, *bottom left and right*). Following the biological example, this creates less opposing moment, which favors the grasping force as the fingers bend. The range of closure is resisted for the 90° bending at both joints. As the joints exceeds the 90° bending the lateral bands move beyond the centre of rotation and start assisting the flexion. This is not the case in this design since the fingers are never meant to bend more than 90°. Note that these flexible elements also have the role of stabilizing the joint for translation and adduction/abduction. The joint stabilizes for hyperextension once the driving system (tendons and whiffle tree mechanism) is assembled.

The mathematical formula describing friction in belt drives (Eq. 1) describes the case of cables moving around fixed circular surfaces. The ratio between the pulling tension in the direction of the moving cable T_2 and the tension at the other end of the surface T_1 depends on the coefficient of friction between the cable and the surface μ_s and the angle of contact Θ . On this basis, a tendon-based driving system that provides a smooth change between the inlet and outlet directions of the pulleys of the phalangeal joints reduces the force loss associated to friction. In other words, the angle Θ

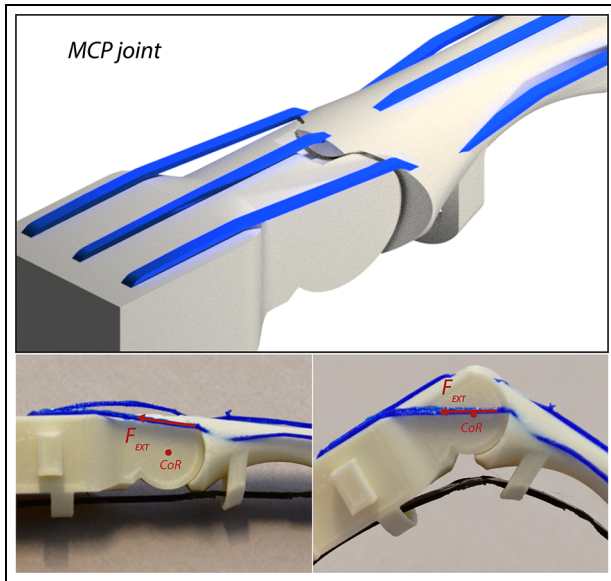


Figure 3. The design of the links and the connections. (Top) The design of the MCP joint with strip elements (“EDC tendons”) in blue. (Bottom left) Note that in the straight configuration, the line of action of the extension force (F_{ext}) is above the center of rotation (CoR) of the MCP joint. (Bottom right) The MCP joint in a flexed configuration; note that the line of action of F_{ext} is closer to the CoR.

should be kept close to 0° (Figure 4, right); this can be achieved by designing a driving “tendon” that bends over predefined points located in the space between pulleys. In these spaces the tendon can bend and follow the shape of the flexing finger while the segments of the tendon in contact with the pulleys remain stiff (difficult to deform), thus preventing sharp bending angles over the pulleys. The dashed lines in Figure 4, right show a tendon with no predefined bending points forming the

angle Θ' . Note that angle Θ' is larger than Θ , indicating less friction force involved. The tendon bending points can be defined by modifying the geometry of the cross-sectional area of the tendon at certain segments (points identified with A and B in Figure 4, left) similar to the flexor tendons in the human hand. These segments have flatter cross-section while the nominal value of the cross-sectional area is kept identical to the rest of the tendon, that is the tendon is flatter but wider at those points. This provides low bending resistance of the cable at those flat points but maintains the same tensile strength at every point of the cable. To reduce the friction even further, the contact surfaces between the cable and the pulleys are rounded to reduce sharp interactions. The pulley therefore has a circular profile to the dorsal direction of the finger (where the pulley is in contact with the tendon), reducing the action of the normal forces on the contacting surfaces.

$$T_2 = T_1 e^{\mu_s \theta} \quad (1)$$

Design choices for 3D printing using the material extrusion technology

An Ultimaker 3 FDM printer utilizing multi-material extrusion technology was used to fabricate the design proposed in this study. This type of FDM process permits the deposition of materials with different mechanical properties. In this way, a material with a low elastic modulus can be 3D printed together with a material with a high elastic modulus. For the manufacturing of each finger, the phalanges (i.e., stiff “bony” parts) were 3D printed using Ultimaker® polylactic acid (PLA) (Ultimaker B.V., Utrecht, The Netherlands), while the connecting parts that keep the joints together (i.e., flexible “ligament” parts) were printed using Ultimaker®

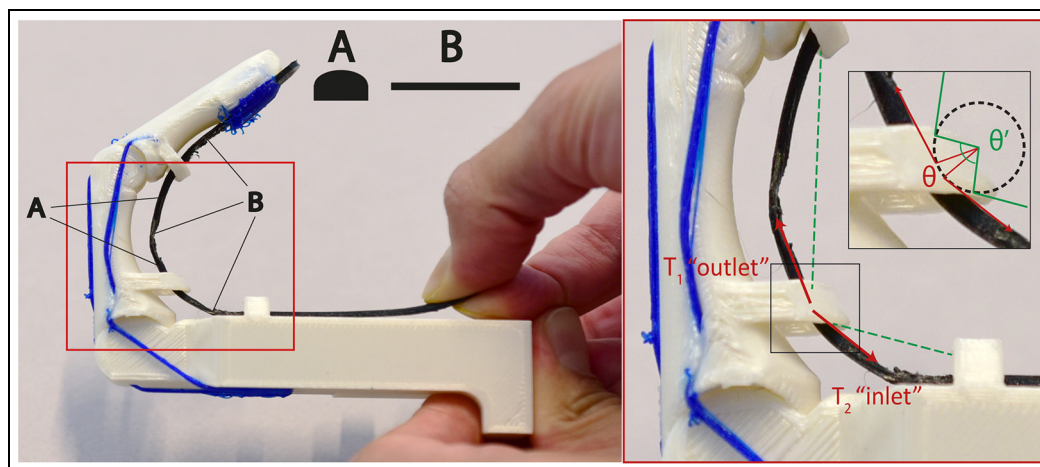


Figure 4. The design of the driving tendon. (Left) A and B represent the corresponding cross-section area at the points indicated by the lines. B is significantly flatter. However, both A and B have the same area. (Right) A close-up view of the pulley at the MCP joint. The angle of contact θ between the cable and the circular surface (pulley) is shown. The dashed points in green indicate the lines of action of T_1 and T_2 if the tendon had the same cross-section area along its full length. The tendon would bend around the shape of the pulley. Note that θ' is larger than θ .

TPU 95A thermoplastic polyurethane (TPU) (Ultimaker B.V., Utrecht, The Netherlands). The design was prepared in such a way that the TPU parts were embedded into the PLA parts during the 3D printing process, thereby creating fully assembled structures. Similarly, the finger pads were also fabricated in TPU together with the phalanges, embedding parts of the finger pads to the distal part of the fingers and thumb. As a soft material, TPU is able to deform elastically around an object's shape when pressed against it, increasing the friction over the finger pads and thereby enhancing grasping.

The parts fabricated in TPU are designed to stretch during maximum flexion before yielding. This elastic deformation provides spring-like behavior that returns the fingers to an extended position. A relatively low cross-section area (1.2 mm^2) is chosen to facilitate bending and tensional deformation. This is an important decision, because the force needed to achieve the flexion of the fingers should be relatively low in order to minimize user fatigue. Furthermore, the lengths of the TPU parts are selected such that sufficient elongation is provided for the full range of motion, while preventing extensions beyond the yield point, i.e. an extension of less than 55%.³⁰

The tendons that comprise the transmission system are 3D printed in Nylon in a second printing job. This material is both strong and ductile, allowing relatively high bending angles without failure, and has a low coefficient of friction.³¹ The nominal cross-section area is set to 4 mm^2 , ensuring sufficient strength to prevent yielding below a tensile load of 110 N per finger (taking the yield stress as 27.8 MPa ³¹). The transmission system can then hold a total activation force of 440 N without risk of failure. This is beyond the average operational forces reported in Hichert et al.³² Additionally, each tendon has a geometrical profile that reduces the interaction with the pulleys to round contacts in order to reduce the friction. The tendons are assembled manually by inserting them through the tip of the finger pads and the pulleys. Once the insertion is completed, the tendon is fixed by mechanical contact between the PP and the head of the tendon. The whiffle tree mechanism is 3D printed in PLA and assembled by manually inserting the four fixation points into the holes at the end of each tendon.

Evaluation methods

The mechanical performance of the hand prosthesis was evaluated using two criteria: (1) the energy employed to execute a pinch grasp and the energy dissipated when the prosthesis opens, and (2) pinch force output due to contact between the thumb, index, and middle fingers. These variables explain how easy it is to operate the prosthetic hand in terms of the user's energy demand and how functional the grasping

function is in terms of the maximum magnitude of the force that can be exerted to an object. For this reason, an experimental setup based on previous work was used.^{8,33} It consists of two load cells and a displacement sensor. A Zemic FLB3G-C3-50 kg-6B (Zemic Europe B.V., Etten-Leur, The Netherlands) load cell was used to measure the input (pulling) force and a FUTEK LLB130 (FUTEK Advanced Sensor Technology Inc, Irvine (CA), USA) load cell housed by a 11 mm-thick cover was used to measure the pinch force. The displacement sensor measures the movement of the cable associated with the activation force of the prosthesis. The hand prosthesis was mounted on the test bench by fixing the palm to the frame and connecting the displacement sensor and the load cells. One load cell was fixed to the thumb's finger pad and the other load cell was connected together with the displacement sensor to the whiffle tree mechanism's driving link via a steel cable. An input force was then exerted to the prosthesis by pulling from the cable. No human subjects were involved to test the hand prosthesis.

The energy dissipated by the prosthesis is obtained by measuring the energy used to close (E_c) the device and the energy returned (E_r) when the fingers open to the initial state. The energy dissipated is then the difference $E_c - E_r$. The energy utilized in each event could be calculated as the integration of the cable forces along their related values of cable excursion. The procedure to measure the variables of interest is described as follows. First a full closing and opening cycle for a pinch grasp (until the index and middle fingers meet the thumb); and second, closing and pinching the pinch load cell until an actuation force of 100 N was reached. Each experiment was repeated five times. An average and a standard deviation were calculated for each variable. Note that the 100 N is applied to the whiffle tree mechanism, which equally divides the force to each moving finger (25 N per finger).

Results

The 3D printed prosthetic hand was fabricated using three materials (i.e., PLA, TPU, and Nylon). The total weight of the device is 92 g and its total material price is ≈ 12 US dollars. The neutral pose of the hand is with the fingers fully extended. The hand is actuated by a conventional pulling cable used in BP prostheses that is connected to the coupling of the whiffle tree mechanism. The whiffle tree mechanism distributes the force to the four tendons which bend all fingers simultaneously as pulled. The hand can perform power, pinch, and tripod grasps as shown in Figure 5. The force versus displacement curve and the pinch force measurements are presented in Figure 6. The energy used to close the prosthesis is $0.380 \text{ Nm} \pm 0.053$ (mean \pm SD) and the energy dissipated is $0.324 \text{ Nm} \pm 0.055$ (mean \pm SD).



Figure 5. The grasping patterns. (top left and right) Pinch grasping, (middle left and right) power grasping, (bottom left and right) and tripod grasping.

The pinch force measured for a 100 N input force is $16.84 \text{ N} \pm 0.88$ (mean \pm SD).

Discussion

The design described in this manuscript demonstrates several bio-inspired design features and was successfully

produced using 3D printing. The device is capable of executing different grasping patterns due to the adaptive grasping provided by the articulated fingers and the whiffle tree mechanism. The assembly of the hand was minimized to two post-processing operations besides the usual support removal after 3D printing: (1) the insertion of the Nylon tendons and (2) the assembly of the force distribution system (i.e., the whiffle tree mechanism). No extra parts or tools were required. The main body of the hand, the phalanges and the connecting elements are 3D printed simultaneously with PLA and TPU taking 20 h of printing time. The four driving tendon elements and the whiffle tree mechanism take 4 h and 3.5 h respectively. The 3D printer was used with the following settings: nozzle diameter: 0.4 mm, layer height: 0.15 mm, and infill: 15%. Assuming a peak power consumption of 221 W (from the technical data-sheet of the manufacturer) the total energy usage can be estimated as 5.97 kWh for a total running time of 27 h. The average electricity price in the Netherlands is 23 cents of euro per kWh, which at the current exchange rate yields a total energy cost of 1.5 US dollars for producing the hand.

The manufacturing advantages of the 3D printing technology were conveniently used to fabricate an assembled mechanical device. Multi-material printing has proven to be particularly advantageous when building parts that are required to present different mechanical properties at different areas. It is worth noting that different combinations can be 3D printed, even if the materials are not bonding properly onto one another during their deposition. In our design two materials (PLA and TPU) can be 3D printed simultaneously, by embedding one of the materials into the other, thereby creating mechanical interlocking. This interlocking can withstand enough loads for the intended purpose because a high stress is never applied to these structures during normal actuation of the hand (less than 90° bending per joint). These embedded parts are only subjected to the load of the TPU strips stretching during the flexion of the finger, which compared to the load at the PLA sliding joints is very low. On the other hand,

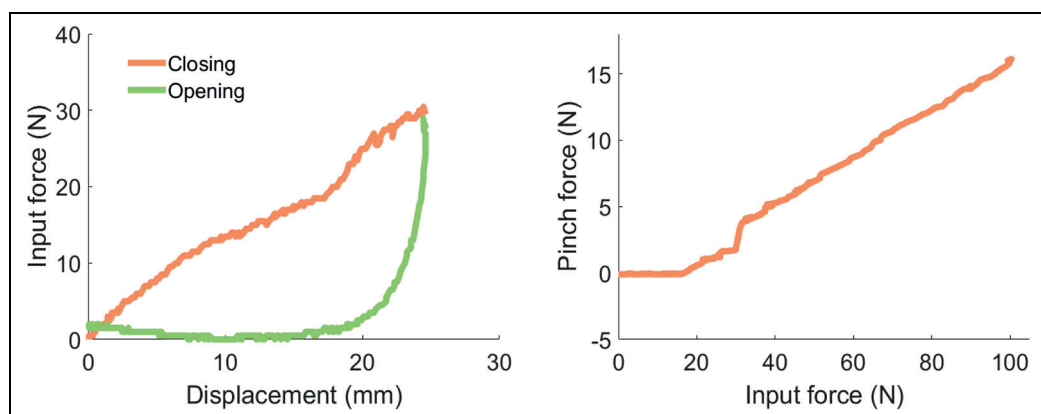


Figure 6. The mechanical test. (Left) Cable displacement versus the input force for a closing-opening cycle. (Right) Input force versus pinch force.

the mechanical properties of these interlocked structures are mostly unknown. We encourage a study of the mechanical properties of the embedded TPU parts in PLA given different geometrical and 3D printing parameters because the mechanical behavior could be optimized and used in future designs and applications.

Surprisingly almost all research describing 3D printed BP hand designs do not report pinch forces.^{5,10,11,13,16,17} Just one other paper reports grasping force measurements of a 3D printed hand (0.5–1 N for precision grasping), but without their corresponding activation forces.³⁴ In our design the pinch force achieved (16.84 N @ 100 N activation force) is superior to other fully 3D printed BP prosthetic hand (~6 N @ 100 N activation force)⁸ but still below that of conventional BP hand prostheses (20–58 N @ 100 N).^{33,35} The commercial BP hands that are usually produced in a factory or a specialized workshop with conventional production processes have a higher pinch force at the same activation force, but are accordingly more expensive and usually heavier and/or have no articulated fingers.³⁵ Due to lack of data regarding the mechanical evaluation of other 3D printed BP hands in the literature, it is impossible to establish direct comparisons.⁵ The increase in the pinch force (> 100%) compared to the current status of a 3D printed prosthesis is, nevertheless, noteworthy. This suggests better grasping and implies superior performance for the activities of daily life. The input force needed to start a pinch grasp (~30 N) and the energy required (0.380 Nm) are however higher than that of the other 3D printed hand (16–18 N, 0.104 Nm, respectively),⁸ but nonetheless lower than most of the conventional BP prosthetic hands (~30–85 N, 0.720–2.292 Nm, respectively).^{33,35} This data indicates that this bio-inspired prosthetic hand is capable of reaching a more suitable pinch force for activities of daily living at the expense of a higher energy cost. Our prosthesis might then be difficult to use for a significant part of the users although our prosthesis requires less activation force and shows better pinch force/actuation force ratio than other conventional prostheses already in the market.^{32,33} The increase of force required compared to the current status of 3D printed hands is therefore problematic and requires further development. A key challenge for the future is then to reduce the activation force and improving the pinch force/actuation force ratio. More testing would be required to evaluate user fatigue, as even though it requires less energy to use than conventional prosthetics, it does require more energy than other 3D printed hands. The implications of this are also user-dependent; contractions up to 15%–20% of a muscle's peak force can be largely fatigue-free,³⁶ meaning the user's physical strength plays a large role in the rate of fatigue. To provide a deeper understanding of the limitations of this design, a functional evaluation involving prosthetic users would be highly desirable.

The amount of energy dissipated (0.324 Nm) suggests a damping-like dynamic of the joint, i.e. most of the energy is dissipated rather than returned (Figure 6, left). This can be explained partly by the friction still remaining in the system and by the nonlinear and/or viscoelastic response of the TPU to strain perturbation. In other words, the motion of the joints depends on the strain rate experience by the TPU strips and thus by the activation velocity of the fingers. As described earlier, the joint is stabilized by TPU strips and the returning forces are provided by their elastic deformations. During the experiment, the tension over the fingers was completely released almost instantly after the pinch grasp was achieved. For different releasing and tension speeds, the response could be significantly different. While the nonlinear mechanical behavior of industrial TPU is well understood,^{37,38} in 3D-printed TPU it is mainly unknown. As manifested in several investigations, 3D printed parts are highly anisotropic and important differences can be found between the standard material and the one used for 3D printing.³⁹ Further investigations on the influence of 3D printing parameters in the mechanical behavior of TPU can provide more understanding of its nonlinear behavior and give better tools to design improved joint connections that reduce the energy dissipation for the current application. Ideally the TPU connecting parts should behave like a spring without damping. Alternatively, other soft material suitable for FDM 3D printing could be explored.

We identified new bio-inspired elements, based on anatomical parts of the human finger, that were successfully incorporated into a prosthetic hand design and manufactured entirely by 3D printing technology. The resulting prosthetic hand is body-powered and has the following features: anthropomorphic shape, light weight, adaptive grasping, articulated fingers, and minimized post-printing assembly. The prosthetic hand is also an accessible option due to its low production cost and is therefore potentially suitable for places where state-of-the-art prosthetic workshops are absent.

Conclusion

A BP prosthetic hand featuring bio-inspired articulated fingers was designed and manufactured via multi-material FDM 3D printing from three materials. The pinch force measurements demonstrate that the prosthetic hand achieves higher forces as compared to other 3D printed prosthetic hands but do not match other BP prosthetic devices. Nevertheless, other advantageous features were included using the unique characteristics of 3D printing technology. This prosthetic hand incorporates new bio-inspired features, is body-powered and has the following characteristics: anthropomorphic shape, light weight, adaptive grasping, articulated fingers, and minimized post-printing

assembly. Summing the relatively low price of the materials, these characteristics make the prosthesis presented in this work a feasible alternative for current solutions in low-income countries.

Acknowledgements

The authors would like to thank the Delft Global Initiative for their financial support and continuous collaboration.

Declaration of conflicting interests

The author(s) declared no potential conflicts of interest with respect to the research, authorship, and/or publication of this article.

Funding

The author(s) disclosed receipt of the following financial support for the research, authorship, and/or publication of this article: This study was supported from the Delft Global Initiative.

ORCID iDs

Juan Sebastian Cuellar  <https://orcid.org/0000-0003-0793-4503>

Gerwin Smit  <https://orcid.org/0000-0002-8160-3238>

References

- Owings MF and Kozak LJ. Ambulatory and inpatient procedures in the United States, 1996. *Vital Health Stat* 1998; 13: 1–119.
- Ziegler-Graham K, MacKenzie EJ, Ephraim PL, et al. Estimating the prevalence of limb loss in the United States: 2005 to 2050. *Arch Phys Med Rehabil* 2008; 89: 422–429.
- Murray C. *Amputation, prosthesis use, and phantom limb pain*. Cham: Springer, 2010, pp.1–203.
- Belter JT, Segil JL, Dollar AM, et al. Mechanical design and performance specifications of anthropomorphic prosthetic hands: a review. *J Rehabil Res Dev* 2013; 50: 599–617.
- Ten-Kate J, Smit G and Breedveld P. 3D-printed upper limb prostheses: a review. *Disabil Rehabil Assist Technol* 2017; 12: 300–314.
- Gibson I, Rosen DW and Stucker B. Introduction and basic principles. In: Gibson I, Rosen DW and Stucker B (eds) *Additive manufacturing technologies*. 1st ed. New York, NY: Springer, 2010, pp.20–35.
- Cuellar JS, Smit G, Plettenburg D, et al. Additive manufacturing of non-assembly mechanisms. *Addit Manuf* 2018; 21: 150–158.
- Cuellar JS, Smit G, Zadpoor A, et al. Ten guidelines for the design of non-assembly mechanisms: the case of 3D-printed prosthetic hands. *Proc IMechE, Part H: J Engineering in Medicine* 2018; 232: 962–971.
- Andrianesis K and Tzes A. Development and control of a multifunctional prosthetic hand with shape memory alloy actuators. *J Intell Robot Syst* 2015; 78: 257–289.
- Bahari MS, Jaffar A, Low CY, et al. Design and development of a multifingered prosthetic hand. *Int J Soc Robot* 2012; 4: 59–66.
- Laliberte T, Baril M, Guay F, et al. Towards the design of a prosthetic underactuated hand. *Mech Sci* 2010; 1: 19–26.
- Gretsch KF, Lather HD, Peddada KV, et al. Development of novel 3D-printed robotic prosthetic for transradial amputees. *Prosthet Orthot Int* 2016; 40: 400–403.
- Zuniga JM, Peck JL, Srivastava R, et al. An open source 3D-printed transitional hand prosthesis for children. *J Prosthet Orthot* 2016; 28: 103–108.
- e-NABLE. The raptor hand. *Enabling the future*. 2014.
- Groenewegen MWM, Aguirre ME and Herder JL. Design of a partially compliant, three-phalanx underactuated prosthetic finger. In: *Proceedings of the ASME design engineering technical conference*, 2–5 August, Boston, MA.
- Alkhatib F, Mahdi E and Cabibihan JJ. Design and analysis of flexible joints for a robust 3D printed prosthetic hand. *IEEE Int Conf Rehabil Robot* 2019; 2019: 784–789.
- Mutlu R, Alici G, in het Panhuis M, et al. 3D printed flexure hinges for soft monolithic prosthetic fingers. *Soft Robot* 2016; 3: 120–133.
- Sharbafi MA, Rode C, Kurowski S, et al. A new biarticular actuator design facilitates control of leg function in BioBiped3. *Bioinspir Biomim* 2016; 11: 046003.
- Lin HT, Leisk GG and Trimmer B. GoQBot: a caterpillar-inspired soft-bodied rolling robot. *Bioinspir Biomim* 2011; 6: 026007.
- Nguyen QV and Chan WL. Development and flight performance of a biologically-inspired tailless flapping-wing micro air vehicle with wing stroke plane modulation. *Bioinspir Biomim* 2019; 14: 016015.
- Scali M, Pusch TP, Breedveld P, et al. Ovipositor-inspired steerable needle: design and preliminary experimental evaluation. *Bioinspir Biomim* 2018; 13: 016006.
- Flinn SR and DeMott L. Functional anatomy. In: Cooper C (ed.) *Fundamentals of hand therapy*. 2nd ed. London: Elsevier, 2014, pp.15–34.
- Toldt C, Dalla Rosa A and Paul E. *An atlas of human anatomy for students and physicians*. New York, NY: Rebman Company, 1919.
- Shrewsbury MM and Kuczynski K. Flexor digitorum superficialis tendon in the fingers of the human hand. *Hand* 1974; 6: 121–133.
- Benjamin M, Kaiser E and Milz S. Structure-function relationships in tendons: a review. *J Anat* 2008; 212: 211–228.
- Hauger O, Chung CB, Lektrakul N, et al. Pulley system in the fingers: normal anatomy and simulated lesions in cadavers at MR imaging, CT, and US with and without contrast material distention of the tendon sheath. *Radiology* 2000; 217: 201–212.
- Plettenburg DH. Basic requirements for upper extremity prostheses: the WILMER approach. In: *Proceedings of the 20th annual international conference of the IEEE engineering in medicine and biology society. Vol. 20 Biomedical engineering towards the year 2000 and beyond (Cat No98CH36286)*. Hong Kong, 1 November 1998, vol. 5, pp.2276–2281. IEEE.

28. Vicinus JH. *X-ray anthropometry of the hand*. Wright-Patterson AFB, OH: Aerospace Medical Research Laboratories, 1962.
29. Chandler R, Clauser C, McConville J, et al. *Investigation of inertial properties of the human body*. Wright-Patterson AFB, OH: Aerospace Medical Research Laboratories, 1975, p.171.
30. Ultimaker. Technical data sheet, TPU, <https://support.ultimaker.com/hc/en-us/articles/360012664440-Ultimaker-TPU-95A-TDS> (accessed 1 December 2020).
31. Ultimaker. Technical data sheet, Nylon, <https://support.ultimaker.com/hc/en-us/articles/360011962600-Ultimaker-Nylon-TDS> (accessed 1 December 2020).
32. Hichert M, Vardy AN and Plettenburg D. Fatigue-free operation of most body-powered prostheses not feasible for majority of users with trans-radial deficiency. *Prosthet Orthot Int* 2018; 42: 84–92.
33. Smit G and Plettenburg DH. Efficiency of voluntary closing hand and hook prostheses. *Prosthet Orthot Int* 2010; 34: 411–427.
34. Alkhatib F, Cabibihan JJ and Mahdi E. Data for benchmarking low-cost, 3D printed prosthetic hands. *Data Brief* 2019; 25: 104163.
35. Smit G, Plettenburg DH and van der Helm FCT. The lightweight Delft Cylinder Hand: first multi-articulating hand that meets the basic user requirements. *IEEE Trans Neural Syst Rehabil Eng* 2015; 23: 431–440.
36. Monod H. Contractility of muscle during prolonged static and repetitive dynamic activity. *Ergonomics* 1985; 28: 81–89.
37. BASF. Thermoplastic polyurethane elastomers, Elastollan[®]—material properties. https://plastics-rubber.basf.com/global/en/performance_polymers/products/elastollan.html (2017, accessed 1 December 2020).
38. Qi HJ and Boyce MC. Stress-strain behavior of thermoplastic polyurethanes. *Mech Mater* 2005; 37: 817–839.
39. Dizon JRC, Espera AH, Chen Q, et al. Mechanical characterization of 3D-printed polymers. *Addit Manuf* 2018; 20: 44–67.